"The Magnetized Interstellar Medium"
8–12 September 2003, Antalya, Turkey
Eds.: B. Uyaniker, W. Reich & R. Wielebinski

Prospects for Polarimetry of the Interstellar Medium with the Planck Satellite

Jan A. Tauber
(on behalf of ESA and the Planck Scientific Collaboration)

Astrophysics Division, Research and Scientific Support Department of the European Space Agency, ESTEC, P.O. Box 299, 2200AG Noordwijk, The Netherlands

Abstract. We present an overview of the European Space Agency's Planck mission, its scientific objectives and the main elements of its technical design. The current programmatic status of Planck within ESA's Scientific Programme, implementation plans, and near-term milestones are also outlined. We place some emphasis on the design of Planck as a polarimeter and we discuss its potential contribution to our knowledge of the magnetized interstellar medium in the Milky Way.

1 Overview

1.1 Scientific objectives

Planck (*http://www.rssd.esa.int/Planck*) is a space observatory designed to image the temperature anisotropies of the Cosmic Microwave Background (CMB) over the whole sky, with unprecedented sensitivity ($\Delta T/T \sim 2 \times 10^{-6}$) and angular resolution ($\sim 5'$). Planck will provide a major source of information relevant to several cosmological and astrophysical issues, such as testing theories of the early Universe and the origin of cosmic structure.

The ability to measure to high accuracy the angular power spectrum of the CMB fluctuations will allow the determination of fundamental cosmological parameters such as the density parameter (Ω_0), and the Hubble constant H_0, with an uncertainty of the order of a few percent (e.g. Bersanelli et al., 1996; Bond et al., 1997; Efstathiou and Bond, 1999). Planck will not only measure the temperature fluctuations of the CMB, but also its polarisation state. This measurement (e.g. Seljak, 1997) will not only yield new scientific results, but will also help to analyze the CMB temperature anisotropies (in particular by resolving degeneracies in the estimation of some cosmological parameters; see Zaldarriaga et al. (1997), Kamionkowski and Kosowsky (1998)).

In addition to the main cosmological goals of the mission, the Planck sky survey will be used to study in detail the very sources of emission which "contaminate" the signal due to the CMB, and will result in a wealth of information on the properties of extragalactic sources, and on the dust, gas, and magnetic field in our own Galaxy (e.g. De Zotti et al., 1999).

1.2 Payload design

The scientific prescription which will allow Planck to meet its ambitious objectives calls for:

- an offset telescope with a physical aperture of size ~ 1.5 m to achieve the angular resolution
- state-of-the-art broadband detectors covering the range ~ 25 to ~ 1000 GHz, to achieve the required sensitivity and the ability to remove foreground sources of emission
- a survey with all-sky coverage carried out from a far-Earth orbit
- extreme attention to rejection of unwanted systematic effects.

To achieve this prescription a payload was conceived for Planck (Bersanelli et al., 1996) consisting of three basic components: (1) a telescope and baffling system, providing the angular resolution and rejection of straylight; (2) a Low Frequency Instrument (or LFI) – an array of tuned radio receivers, based on HEMT amplifiers, covering the frequency range 25–110 GHz, and operated at a temperature of 20 K; and (3) a High Frequency Instrument (or HFI), consisting of an array of bolometers operated at 0.1 K and covering the frequency range 90–1000 GHz.

The major elements of the Planck payload and their disposition on the spacecraft can be seen in Figures 1 and 2.

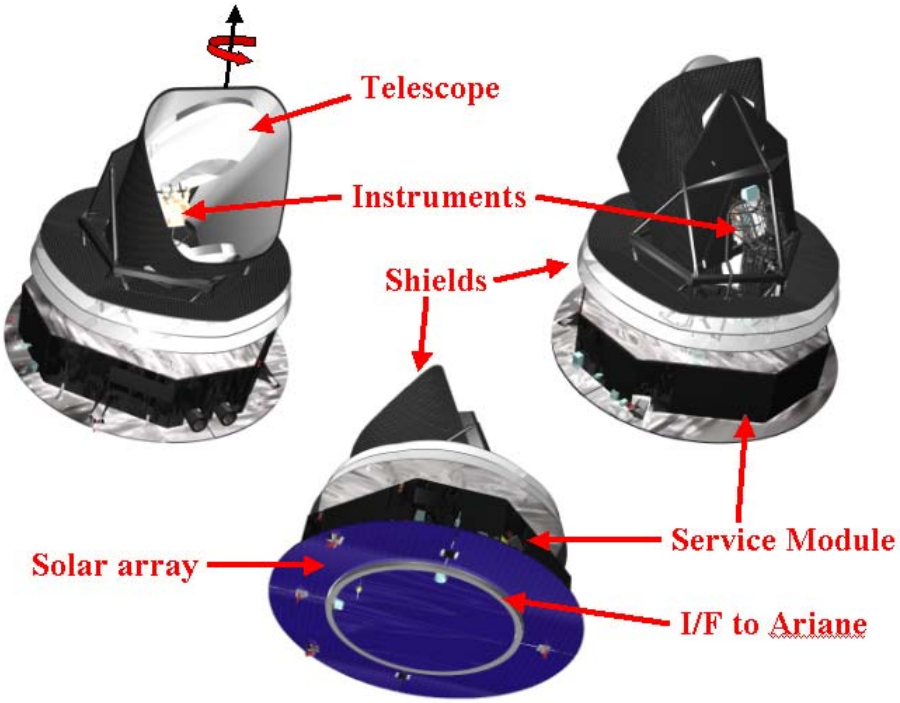

Fig. 1. A conceptual view of the arrangement of the main elements of the Planck payload. The instrument focal plane unit contains both low and high frequency detectors. The function of the large shield surrounding the telescope is to control the far sidelobe level of the radiation pattern as seen from the detectors. Specular cones thermally decouple the Service Module (located below the payload) from the Payload Module, and allow the payload environment to reach its nominal temperature of ~ 50 K. The satellite's spin axis is indicated; the Sun is always kept in the anti-spin direction (perpendicular to the solar array). The satellite views are courtesy of Alcatel Space (Cannes).

1.3 Programmatic aspects

Planck was selected in 1996 as the third Medium-Sized Mission (M3) of ESA's Horizon 2000 Scientific Programme; today it is part of ESA's Cosmic Visions programme. Planck was formerly called COBRAS/SAMBA. After the mission was selected and approved (in late 1996), it was renamed in honor of the German scientist Max Planck (1858–1947), Nobel Prize in Physics in 1918. Planck will be launched together with ESA's Herschel Far-Infrared and Submillimetre Space Observatory in February 2007.

Starting in 1993, a number of technical studies laid the basis for the issue in September 2000 of an Invitation to Tender (ITT) to European industry for the procurement of the Herschel and Planck spacecraft. From the submitted proposals, a single prime contractor, Alcatel Space (France), was selected in early 2001 to develop both Herschel and Planck spacecrafts. Alcatel Space is supported by two major subcontractors: Alenia Spazio (Torino) for the Service Module, and Astrium GmbH (Friedrichshafen) for the Herschel Payload Module; and by many other industrial sub-contractors

from all ESA member states. The detailed definition work began in June 2001, and is very advanced at the time of writing. A view of the current design of Planck is shown in Figure 1.

Planck is a survey-type project which is being developed and operated as a Principal Investigator mission. In early 1999, ESA selected two Consortia of scientific institutes to provide the two Planck instruments: the Low Frequency Instrument will be developed and delivered to ESA by a Consortium led by Reno Mandolesi of the Istituto di Astrofisica Spaziale e Fisica Cosmica (CNR) in Bologna (Italy); similarly, the High Frequency Instrument will be provided to ESA by a Consortium led by Jean-Loup Puget of the Institut d'Astrophysique Spatiale (CNRS) in Orsay (France). More than forty European institutes, and some from the USA, are collaborating on the development, testing, and operation of these instruments, as well as the ensuing data analysis and exploitation. The currently foreseen capabilities of the instruments are described in Table 1; more detailed recent descriptions can be found in Mandolesi et al. (2003; LFI) and Lamarre et al. (2003; HFI).

In early 2000, ESA and the Danish Space Research Institute (DSRI, Copenhagen) signed an Agreement for the provision of the two reflectors that constitute the Planck telescope. DSRI leads a Consortium of Danish institutes, and has subcontracted the development of the Planck reflectors to Astrium GmbH (Friedrichshafen), who are manufacturing the reflectors using state-of-the-art carbon fibre technology.

The instrument development has proceeded largely according to schedule, in spite of a number of financial difficulties during 2002, which at the time of writing have been resolved. Hardware subsystems are already being manufactured and tested. The first deliveries of instrument qualification models are expected in mid-2004, with the flight models due in mid-2005.

2 Scientific performance

The principal objective of Planck is to produce maps of the whole sky in nine frequency channels. The currently foreseen characteristics of the two Planck instruments (see Figure 2) are summarized in Table 1; these characteristics largely drive the quality of the final maps.

Table 1. The currently foreseen characteristics of the Planck payload

Telescope	1.5 m (proj. apert.) Aplanatic; Temp. ∼50 K; $\epsilon_{\rm system} \sim 1\%$								
	Shared focal plane; viewing direction offset 85^o from spin axis								
Instrument	LFI			HFI					
Center Frequency (GHz)	30	44	70	100	143	217	353	545	857
Detector Technology	HEMT receiver arrays			Bolometer arrays					
Detector Temperature	∼20 K			0.1 K					
Cooling Requirements	H_2 sorption cooler			H_2 sorption+4K J-T active stage+^{3}He-^{4}He Dilution					
No. of Unpolarised Detectors	–	–	–	–	4	4	4	4	4
No. of Linearly Polarised Detectors	4	6	12	8	8	8	8	–	–
Bandwidth ($\Delta\nu/\nu$)	0.2	0.2	0.2	0.33	0.33	0.33	0.33	0.33	0.33
Angular Resolution (arcmin)	33	24	14	9.2	7.1	5.0	5.0	5.0	5.0
Average $\Delta T/T$ per pixel (Stokes I) (12 mos., 1σ, 10^{-6} units)	2.0	2.7	4.7	2.5	2.2	4.8	14.7	147.0	6700
Average $\Delta T/T$ per pixel (Stokes U,Q) (12 mos., 1σ, 10^{-6} units)	2.8	3.9	6.7	4.0	4.2	9.8	29.8	–	–

These maps will not only include the CMB itself, but also all other astrophysical foregrounds, whether galactic (free-free, synchrotron or dust) or extragalactic in origin. All nine Planck sky maps will be used to produce a single map of the Cosmic Microwave Background anisotropies. The key that allows to reach this objective is the wide spectral coverage achieved by Planck. Each astrophysical

foreground has a distinct spectral characteristic; specialized data processing algorithms (e.g. Tegmark, 1997; Hobson et al., 1998; Bouchet and Gispert, 1999) will use this information to iteratively extract the signal due to each foreground component, until only the CMB signal remains.

Instrumental systematic effects (e.g. Delabrouille, 1998; Burigana et al., 1998; Maino et al., 1999), as well as uncertainties in the recovery of parameters characterizing the foregrounds will degrade the final noise level in the CMB maps. Therefore the final scientific performance of the mission depends not only on the instrumental behavior, but also on the detailed nature of the various astrophysical foregrounds, the behavior of many systematic effects which produce spurious signals (such as stray-light), and the ability to remove these signals from the measured data by means of data processing algorithms. Current estimates of the performance of Planck are based on simulations of the measurement process (e.g. Bersanelli et al., 1996; Bouchet and Gispert, 1999; Knox, 1999; Tegmark et al., 2000), which include such effects to the best of available knowledge, as well as of the signal extraction process. These simulations suggest that the ability to extract the CMB signal from the measurements will be limited mainly by the background of noise originating in unresolved structure in the various foregrounds.

The Planck instruments are also designed to provide information on the polarisation state of the CMB. Although simulations of the extraction of polarisation from Planck are at a less sophisticated level than those dealing with temperature anisotropies, it is expected that Planck will be able to measure with good accuracy the angular power spectrum of the "E-component" of CMB polarisation (Hu and White, 1997), with the consequent improved estimation of cosmological parameters (Bouchet et al., 1999; Prunet et al., 2000). A detection of the "B-component" should also be achieved (Hu, 2002).

Naturally, as a by-product of the extraction of the CMB, Planck will also yield all-sky maps of all the major sources of microwave to far-infrared emission, opening a broad expanse of astrophysical topics to scrutiny. In particular, the physics of dust at long wavelengths and the relative distribution of interstellar matter (neutral and ionized) and magnetic fields will be investigated using dust, free-free and synchrotron maps. In the field of star formation, Planck will provide a systematic search of the sky for dense, cold condensations which are the first stage in the star-formation process. One specific and local distortion of the CMB which will be mapped by Planck is the Sunyaev–Zeldovich (SZ) effect arising from the Compton interaction of CMB photons with the hot gas of clusters of galaxies (Aghanim et al., 1997; Pointecouteau et al., 1998). The very well defined spectral shape of the SZ effect allows it to be cleanly separated from the primordial anisotropy. The physics of gas condensation in cluster-size potential wells is an important element in the quest to understand the physics of structure formation and ultimately of galaxy formation.

Therefore, even though that is not its primary scientific objective, Planck will deliver high-quality all-sky maps of all extended foreground emission components between cm and submm wavelengths. These maps will constitute a scientific product which is comparable to the IRAS and COBE-DIRBE maps at shorter wavelengths. The high-resolution all-sky nature of the maps, coupled with the broad spectral coverage and highly accurate calibration, will present a unique opportunity to explore in a global sense all the extended emission components of our own as well as external galaxies.

3 Polarimetry with Planck

The Planck instruments were not originally designed to measure polarisation, though they were always based on linearly polarised detectors. However, since its selection, there has been a growing realisation of the scientific importance of measuring the polarisation state of the CMB. Therefore a number of design changes have been made in the past few years to allow Planck to better exploit its existing capabilities. Still, its operation as a polarimeter remains non-standard, and is therefore addressed here in some detail.

The LFI is based on the coherent amplification of radiation collected by a corrugated feedhorn from the telescope and delivered to a Low-Noise Amplifier, for eventual detection after several amplification stages. An Ortho-Mode Transducer located behind the corrugated feedhorn selects two orthogonal linearly polarised modes and feeds them to independent amplification chains. Therefore in the LFI each

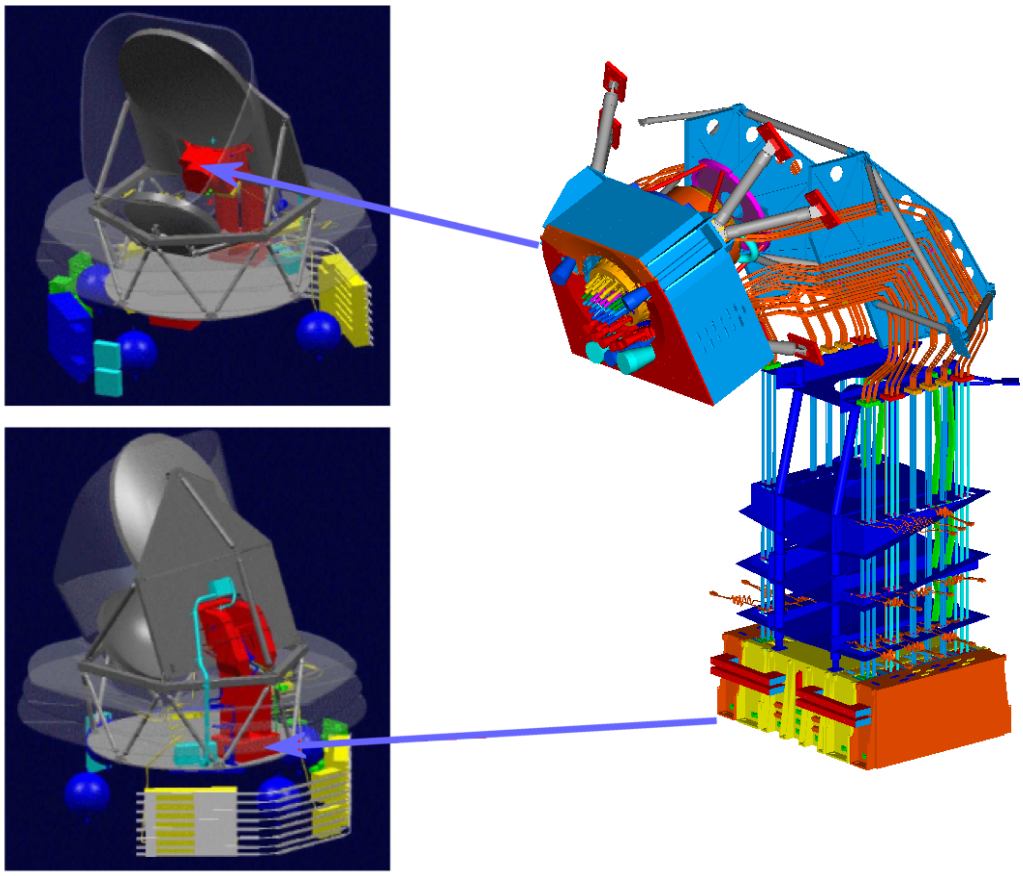

Fig. 2. On the right (top) is shown the combined focal plane unit formed by the LFI and HFI; the colors on each horn correspond to frequency channels. The HFI focal plane is inserted into the ring formed by the LFI horns, and includes thermal stages at 20 K, 4 K, 2 K and 0.1 K. The LFI horns and detectors are cooled to 20 K, and are attached by waveguides to a lower unit containing back-end amplifiers; a complex mechanical structure stiffens the assembly. On the left is shown the manner in which the various instrument units are distributed throughout the Payload and Service Modules. In general all cryogenic units are located in the Payload Module and all warm units (electronics, coolers) are located in the Service Module. The figures are courtesy of Alcatel Space (Cannes) and Laben (Milano).

horn is coupled to two orthogonal polarisations on the sky. The two measurements are independent and allow to determine two Stokes parameters, e.g. I and Q. If an additional horn/OMT/amplification unit is rotated by 45° (around the horn axis) and is pointed to the same part of the sky, the four measurements together allow to determine three Stokes parameters, I, Q, and U.

The principle of Planck polarimetry consists of a focal plane design (see Figure 3) that allows each part of the sky to be measured by two horns (four detectors, sampling all polarisation directions spaced by 45°). This is achieved by placing pairs of horns in the focal plane in such a way that they follow the same path on the sky, acquiring data on the same pixels with a small time delay. Each detector (of a set of at least four) is sampled independently, and post-processing on the ground ensures that I, Q, and U are recovered. The last Stokes parameter (V, parametrising circular polarisation), is not measured by Planck, but at the same time is not expected to be present in the CMB signals.

The above principle also applies to the HFI. As for the LFI, the radiation is collected by a corrugated feedhorn. However, in this case, it is delivered directly to incoherent detectors, so-called Polarisation Sensitive Bolometers (Jones et al., 2003). These consist essentially of grids of parallel wires which couple to one linear polarisation only; the energy of the radiation absorbed by the grid is dissipated as heat that increases the temperature of a solid-state thermometer. In each horn are

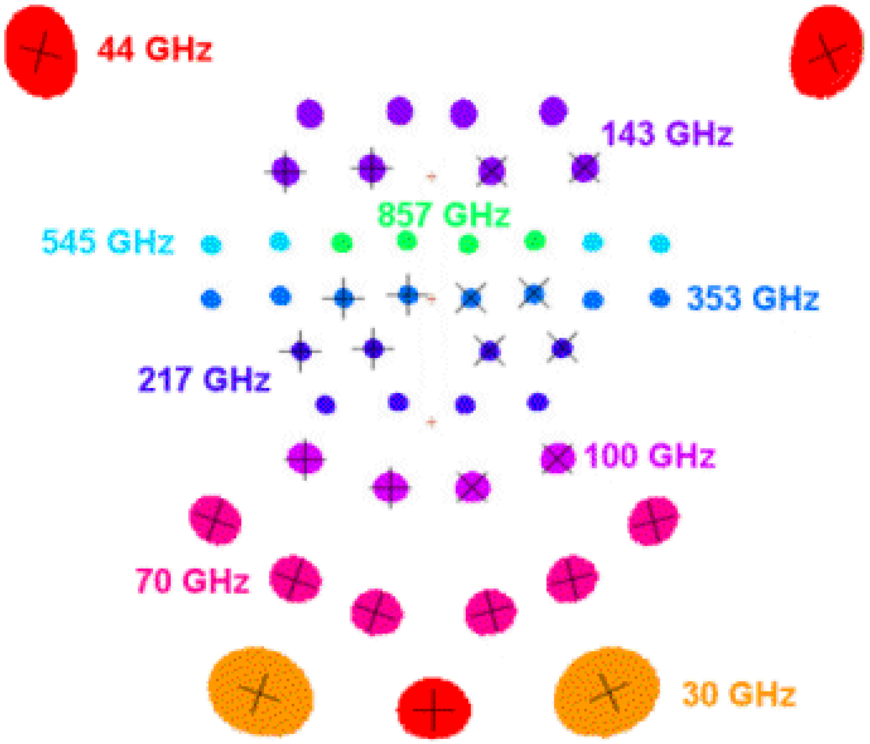

Fig. 3. The footprint of the Planck focal plane on the sky. Each spot corresponds to the −10 dB contour of the beam pattern of each single horn; each frequency is color-coded. The black crosses correspond to the directions of linear polarisation of each pair of detectors supported by the horn. In this diagram the beams are scanned by the satellite in a horizontal direction. Each horn is followed on its scan path by (at least) a second horn, whose directions of polarisation are rotated by 45°. Using this scheme, Planck can measure three Stokes parameters (I, Q, and U).

located two perpendicular grids which allow the independent detection of two orthogonal linear polarisations. Note that not all HFI channels allow polarisation measurements: the two highest frequencies have been designed to support multi-moded operation, which make them intrinsically unsuited to cleanly propagate linearly polarised modes; they contain instead standard ("spider-web") bolometers which absorb simultaneously all polarisations of incident radiation.

A number of systematic effects will be present in the Planck polarisation measurements, which are specific to the measurement method. These systematics originate in the optics of the detector–feedhorn–telescope combination, in receiver-specific effects (such as mismatches between the properties of each detector within a set), thermal effects, calibration effects, and effects due to the scan strategy. These effects are currently under detailed analysis to estimate their impact on the recovery of CMB polarisation information (Leahy et al., 2002; Leahy et al., 2004). Their impact on the recovery of galactic emission polarisation is expected to be much less than for the CMB, given the much larger signal levels expected.

4 Planck and the Magnetized Interstellar Medium

Planck's ability to measure polarisation over a wide frequency range and over the whole sky will be of great use for the determination of magnetic field levels and directions, both within nearby objects and at galactic scales. Planck's unique strength is its ability to probe the same underlying magnetic field simultaneously via its effect on two physically different coupling mechanisms, which operate in two largely non-overlapping frequency ranges.

The presence of magnetic fields in the ISM leaves an imprint in the polarisation characteristics

of its emission. The two important coupling mechanisms are synchrotron and thermal dust emission. Synchrotron emission, discussed extensively in these proceedings, results from the interaction of cosmic-ray electrons with a magnetic field and is strongly polarised and sensitive to both the magnitude and direction of the magnetic field. Thermal dust emission can be polarised depending on the properties of the grains and their level of alignment to the magnetic field.

Until recently, surveys of synchrotron emission have been carried out from the ground, however they are either at very low frequencies where Faraday rotation erases much of the useful information on the large-scale galactic magnetic field, or covering very limited areas within the Galactic plane. The situation has recently changed since the WMAP satellite (Bennett et al., 2003, *http://lambda.gsfc.nasa.gov*) has mapped CMB and galactic emission over the whole sky between 20 and 90 GHz; it is expected that polarisation maps will be released by WMAP very soon to the public. The main (future) advantage of Planck at these lower frequencies will be its much higher sensitivity (nominally a factor of ~ 5).

At higher frequencies, where most of the information related to dust polarised emission resides, the panorama is currently much less well covered, with only limited areas of the galactic plane having been surveyed by recent balloon experiments (Boomerang: Montroy et al., 2003; Archeops: Benoit et al., 2003), and a few pointed high-resolution observatins of nearby dense objects. In this region Planck will be probing a virtually unexplored region.

In the above light, the prospects are very good for Planck to make a very significant impact on the study of the magnetic field within the Milky Way, both at galactic scales and in nearby objects. To achieve this, it will be necessary to use not only the Planck data, but in addition a host of ancillary (continuum and line-emission) data at many frequencies, that will allow to disentangle the various contributors to the various components of galactic emission. The data reduction effort needed to recover the magnetic field information will therefore be major, and is the object of specific ongoing preparations within the Planck collaboration.

5 Mission profile

Planck will be launched together with Herschel in February 2007 by an Ariane 5 rocket from the European spaceport in Kourou (French Guiana). Planck and Herschel will separate immediately after launch, and each will proceed independently to different orbits around the L2 point of the Earth–Sun system. At this location, the payload can be continuously pointed in the anti-Sun direction, thus minimizing potentially confusing signals due to thermal fluctuations and straylight entering the detectors through the far sidelobes.

The transit time for Planck will be between 3 and 4 months; this period will be used for commissioning of the spacecraft and instruments. The spacecraft (S/C) will be placed into a Lissajous orbit around L2 characterised by a $\sim$ 4-month period and a maximum elongation from L2 of about 380000 km, such that the Sun–S/C–Earth angle will not exceed 15°. From this orbit, Planck will carry out two complete surveys of the full sky, for which it requires between 12 and 14 months of observing time.

The satellite will rotate at 1 rpm around a spin axis pointed within 10° of the Sun. The payload will always remain in the shadow of the Sun. The solar array ensures this as long as it is inclined with respect to the Sun–S/C line by less than 10°. The Planck telescope and focal plane define a sparsely sampled field of view (FOV) approximately 8° in diametre (see Figure 3) around a reference line-of-sight which is inclined by 85° with respect to the spin axis. As the satellite rotates, the FOV will thus trace a circle of diametre 170° on the sky.

In order to carry out its two consecutive full-sky surveys and maintain the payload in the solar shadow, the spin axis of Planck must be displaced on the average by 1° per day in the direction defined by the orbital motion of the Earth around the Sun. This is achieved by spin axis depointing manoeuvers at regular intervals. As the spin axis is displaced, the observed circle also moves and gradually covers a large fraction of the sky.

Planck will dump each day to Earth within a period of 3 hours the data acquired during 24 hours. Observations will not be interrupted during the downlink period, and the S/C will not be reoriented towards the Earth. The telemetry antenna is designed to have adequate gain within a 15° half-cone

from the spin axis, ensuring that even at the extremes of its orbit the Planck telemetry can achieve full bandwidth.

6 Operations and data processing

The Planck spacecraft will be controlled from a dedicated Mission Operations Centre developed and operated by ESA in Darmstadt (Germany). From there, the scientific data produced by Planck will be piped daily to two Data Processing Centres (DPCs), which will be developed and operated by the two Consortia selected to provide the Planck instruments.

In particular, the two DPCs will be responsible for:

(a) daily and long-term analysis of instrument health and performance;

(b) daily analysis of science data;

(c) all levels of processing of Planck data, from raw telemetry to deliverable scientific products.

The two DPCs will share a basic information management infrastructure, the Planck Integrated Data and Information System (IDIS, Bennett et al., 2000). IDIS is being conceived from an object-oriented point of view, and is planned to contain five different components:

(a) a Document Management Component, containing all relevant documentation;

(b) a Software Management Component, encompassing the software in common between the two Consortia;

(c) a Process Coordinator Component, providing a single software environment for data processing (e.g. a data pipeline manager);

(d) a Data Management Component, allowing the ingestion, efficient management and extraction of the data (or subsets thereof) produced by Planck activities;

(e) a Federation layer, providing inter-connection among IDIS components (e.g. relating objects controlled by each component).

The main scientific products of the mission will be produced by the two DPCs jointly, and will consist of all-sky maps in ten frequency bands, which will be made publicly available one year after completion of the mission (i.e. in late 2010), together with a first generation set of maps of the CMB, Sunyaev–Zeldovich effect, galactic emission (dust, free-free, and synchrotron), and point-source catalogs. The time series of observations (after calibration and position reconstruction) will also eventually be made available as an on-line archive.

7 Conclusions

Planck is the next quantum step in Cosmic Microwave Background research and is now in full development towards fulfilling its main cosmological objectives. At the same time, the all-sky maps of Planck will constitute a unique opportunity to carry out new and fundamental research on our Galaxy with unprecedented observational advantages: broad spectral coverage (including completely new frequency windows), ability to measure polarised emission, high sensitivity, high photometric accuracy, high spatial resolution especially at the shortest wavelengths, and full-sky coverage. These characteristics will enable detailed and global studies of the components, physical conditions and spatial distribution of the gas and dust in the Milky Way. The ability to measure polarisation will allow to estimate the morphology and characteristics of the galactic magnetic field both at small and large scales. A particular strength in this respect is its broad frequency range, which allows it to probe simultaneously two different mechanisms coupling the magnetic field to the emission. However, specific techniques to reduce the Planck data and correlate it with a host of other tracers of the galactic Interstellar Medium and Magnetic Field still need to be developed, to allow to exploit fully in this respect the Planck database.

Acknowledgments

Planck (*http://astro.esa.int/Planck*) is an ESA project with instruments funded by ESA member states (in particular the PI countries: France and Italy), and with special contributions from Denmark and NASA (USA). This paper draws widely from the work carried out in the past years by the Planck Instrument and Reflector Provider Consortia, ESA, and industry (principally Alcatel Space Cannes).

References

Aghanim, N., de Luca, A., Bouchet, F. R. et al. (1997) *Astron. Astrophys.* **325**, 9.
Bennett, C.L., Banday, A. J., Gorski, K.M. et al. (1996) *Astrophys. J.* **464**, L1.
Bennett, C.L. et al. (2003) *Astrophys. J. Suppl.* **148**, 1.
Bennett, K., Pasian, F., Sygnet, J.F. et al. (2000) *Proc. SPIE* **4011**, 2–10.
Benoit, A., Ade, P., Amblard, A. et al. (2003) in press (astro-ph/0306222).
Bersanelli, M., Bouchet, F.R., Efstathiou, G. et. al. (1996) ESA D/SCI(96)3.
Bond, J.R., Efstathiou, G., Tegmark, M. (1997) *Mon. Not. R. Astron. Soc.* **291**, L33.
Bouchet, F., Gispert, R. (1999) *New Astronomy* **4**, 443.
Bouchet, F.R., Prunet, S., Sethi, S.K. (1999) *Mon. Not. R. Astron. Soc.* **302**, 663.
Burigana, C., Maino, D., Mandolesi, N. et al. (1998) *Astron. Astrophys. Suppl.* **130**, 551.
Delabrouille, J. (1998) *Astron. Astrophys. Suppl.* **127**, 555.
De Zotti, G., Toffolatti, L., Argüeso, F. et al. (1999) in *3 K Cosmology: EC–TMR Conference*, eds. L. Maiani, F. Melchiorri, N. Vittorio, AIP Conf. Ser. **476**, p. 204.
Efstathiou, G., Bond, J.R. (1999) *Mon. Not. R. Astron. Soc.* **304**, 75.
Hobson, M.P., Jones, A.W., Lasenby, A.N. et al. (1998) *Mon. Not. R. Astron. Soc.* **300**, 1.
Hu, W. (2002) *Phys. Rev.* D **65**, 02.
Hu, W., White, M. (1997) *New Astronomy* **2**, 323.
Jones, W.C., Bhatia, R.S., Bock, J.J., Lange, A.E. (2003) in *Millimeter and Submillimeter Detectors for Astronomy*, eds. T.G. Phillips, J. Zmuidzinas, Proc. SPIE **4855**, p. 227.
Kamionkowski, M., Kosowsky, A. (1998) *Phys. Rev.* D **57**, 685.
Knox, L. (1999) *Mon. Not. R. Astron. Soc.* **307**, 977.
Lamarre, J.M, Puget, J.L., Bouchet, F. et al. (2003) *New Astron. Rev.* **47**, 1017.
Leahy, J.P., Yurchenko, V., Hastie, M.A. et al. (2002) in *Astrophysical Polarized Backgrounds: Workshop on Astrophysical Polarized Backgrounds*, eds. S. Cecchini, S. Cortiglioni, R. Sault, and C. Sbarra, AIP Conf. Proc. **609**, p. 215.
Leahy, J.P., Hamaker, J., Tauber, J. (2003), in preparation.
Maino, D., Burigana, C., Maltoni, M. et al. (1999) *Astron. Astrophys. Suppl.* **140**, 383.
Mandolesi, N., Morgante, G., Villa, F. (2003) in *IR Space Telescopes and Instruments*, ed. J. C. Mather, Proc. SPIE **4850**, p. 722.
Mather, J., Fixsen, D.J., Shafer, R.A. et al. (1999) *Astrophys. J.* **512**, 511.
Montroy, T., Ade, P.A.R., Balbi, A. et al. (2003) *New Astron. Rev.* **47**, 1057.
Pointecouteau, E., Giard, M., Barret, D. (1998) *Astron. Astrophys.* **336**, 44.
Prunet, S., Sethi, S.K., Bouchet, F.R. (2000) *Mon. Not. R. Astron. Soc.* **314**, 348.
Revenu, B., Kim, A., Ansari R. et al. (2000) *Astron. Astrophys. Suppl.* **142**, 499.
Seljak, U. (1997) *Astrophys. J.* **482**, 6.
Tegmark, M. (1997) *Astrophys. J.* **480**, L87.
Tegmark, M., Eisenstein, D.J., Hu, W., De Oliveira-Costa, A. (2000) *Astrophys. J.* **530**, 133.
Zaldarriaga, M., Spergel, D.N., Seljak, U. (1997) *Astrophys. J.* **488**, 1.

"The Magnetized Interstellar Medium"
8–12 September 2003, Antalya, Turkey
Eds.: B. Uyaniker, W. Reich & R. Wielebinski

Observations in the BOOMERanG Field at 1.4 GHz

E. Carretti[1], G. Bernardi[1,2], S. Cortiglioni[1], R.J. Sault[2], M.J. Kesteven[2] and S. Poppi[3]

[1]IASF/CNR Bologna, Via Gobetti 101, I-40129 Bologna, Italy
[2]ATNF/CSIRO, P.O. Box 76, Epping, NSW, 1710, Australia
[3]IRA/CNR Bologna, Via Gobetti 101, I-40129 Bologna, Italy

Abstract. The synchrotron emission is expected to be the most important Galactic foreground noise for measurements of the polarization of the Cosmic Microwave Background (CMBP) and the identification of sky areas with low polarized emission by this contaminant is crucial. Observations at low radio frequencies allow both the definition of target regions for deep observations and the estimate of the residual contamination in the frequency range typical of CMBP experiments (30–150 GHz). We present the first observation of the diffuse polarized synchrotron radiation of a patch (about $3^\circ \times 3^\circ$) in the BOOMERanG field, one of the areas with the lowest foreground emission in total intensity. The work has been carried out with the Australia Telescope Compact Array at 1.4 GHz with $3\farcm4$ resolution. The mean polarized signal has been found to be $I^p_{\rm rms} = \sqrt{(Q^2_{\rm rms} + U^2_{\rm rms})} = 11.6 \pm 0.6$ mK, nearly one order of magnitude below that in the Galactic Plane. Extrapolations to frequencies of interest for cosmological investigations suggest that the detection of the CMBP E-mode should be accessible with no relevant foreground contamination at 90 GHz and even the B-mode detection for $T/S > 0.01$ is not ruled out.

1 CMBP and Foreground Contamination

Most of the information we have about the formation and the evolution of the Universe come from Cosmic Microwave Background (CMB) features like anisotropy and polarization. While the anisotropy has been extensively studied by both space (COBE-DMR, WMAP and the planned PLANCK) and ground experiments (BOOMERanG, MAXIMA and DASI among others), the investigation of the polarization is just at the beginning with the first detections of DASI (E-mode signal, Kovac et al. 2002) and WMAP (temperature–E-mode cross-spectrum C^{TE}, Kogut et al. 2003) and still far from a full characterization.

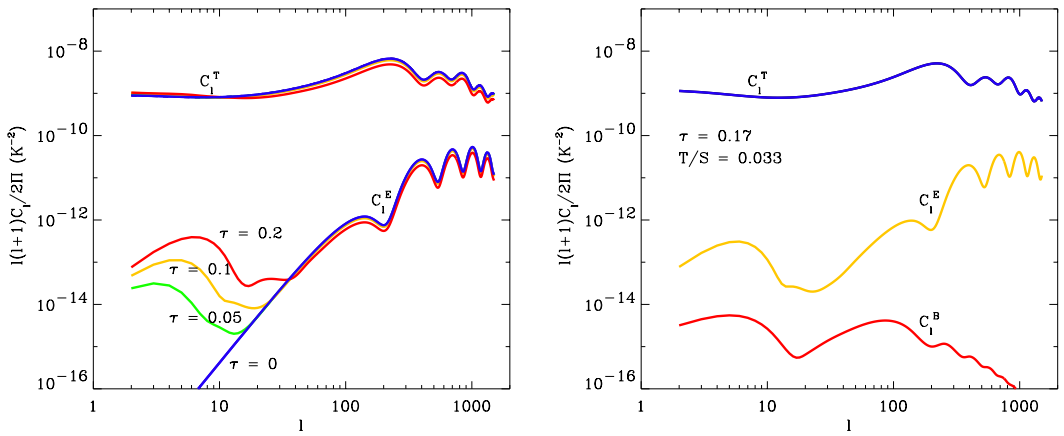

Fig. 1. Left: CMB anisotropy (C^T_ℓ) and E-mode polarization (C^E_ℓ) angular power spectra for a few values of the optical depth τ to the CMB of the re-ionized medium. The other cosmological parameters are those of the *Concordance Model* as from WMAP data (Spergel et al. 2003). Right: B-mode power spectrum of the same model for a tensor to scalar perturbation power ratio $T/S = 0.033$. τ is set to the WMAP best-fit value (Kogut et al. 2003)

The Polarization of the CMB (CMBP) brings us new information with respect to the anisotropy on both large and small angular scales. On large angular scales (multipoles $\ell < 10$, the multipole–angular-scale relation being $\theta = 180°/\ell$) the Angular Power Spectrum (APS) of CMBP is highly sensitive to the presence of a re-ionized medium at the epoch of formation of the first stars and galaxies (Figure 1), and provides information on both the epoch of formation of the first structures and the re-ionization history of the Universe.

On sub-degree scales ($\ell = 200$–1500) the inflationary frame predicts a well-defined peak pattern of the E-mode APS, with minima corresponding to maxima of anisotropy and reverse, and a precise measurement of this pattern would be an important check of the Inflation paradigm (Kosowsky 1999).

In addition, the tensorial perturbations of the gravitational wave background generated by Inflation grows up the faint B-mode (Figure 1) giving us the exciting possibility to make a direct measurement of the energy density of the Universe when Inflation occurred (Kamionkowski & Kosowsky 1998).

In spite of its importance the CMBP signal is faint, expecially the B-mode expected to be two–three (or more) orders of magnitude weaker than the E-mode, depending on the value of the tensor to scalar perturbation power ratio T/S. This calls for searching the CMPB emission in sky regions as free as possible from Galactic foreground contamination.

Among the several components of this foreground noise (synchrotron, free-free, thermal and spinning dust), the free-free emission is expected to be practically unpolarized and hence not relevant, while the spinning dust seems to be ruled out by WMAP results (Bennett et al. 2003). The synchrotron emission is thus expected to be the dominant foreground disturbance up to ~ 100 GHz (see Figure 2) and its study and characterization are mandatory to allow a reliable measurement of CMBP.

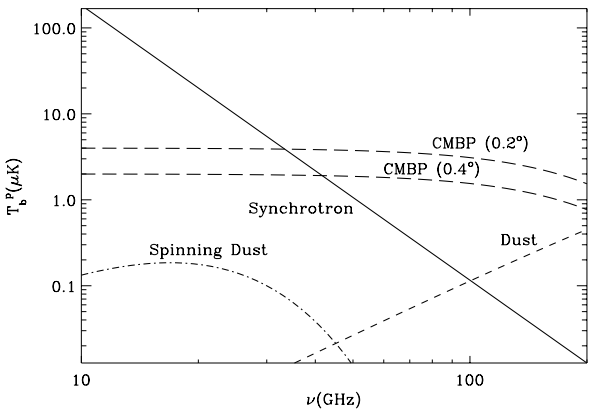

Fig. 2. Polarized emission estimates for the main Galactic foregrounds. The synchrotron component has been normalized to the WMAP results at 23 GHz (Bennett et al. 2003) and assuming 20% polarization. The spectral index is $\beta = -3.2$ as provided by Bennett et. (2003) between 23 and 41 GHz. The thermal dust is modelled with the shape and normalization provided by WMAP data and assuming 1% polarization of the MID model of Tegmark et al. (2000). Finally, for the spinning dust we consider the upper limit provided by WMAP ($< 5\%$ of the total foreground emission at 33 GHz) and assuming the shape and the polarization degree (5%) of Tegmark et al. (2000). CMBP mean emission levels at two angular scales are also reported.

2 Observations of a Low Synchrotron Emission Area

For several reasons balloon-borne and ground-based experiments limit the investigation of the CMBP signal on small patches of the sky (typically $10° \times 10°$) and are devoted to search for the sub-degree emission.

An important task is to identify patches with low foreground emission and characterize them to evaluate the degree of contamination on the CMBP signal.

The southern target of the BaR-SPOrt experiment (Cortiglioni et al. 2003) has been identified using the Rhodes/HartRAO 2326 MHz radio continuum survey (Jonas et al. 1998) where the region already observed by the BOOMERanG experiment (de Bernardis et al. 2000) looks as the lowest

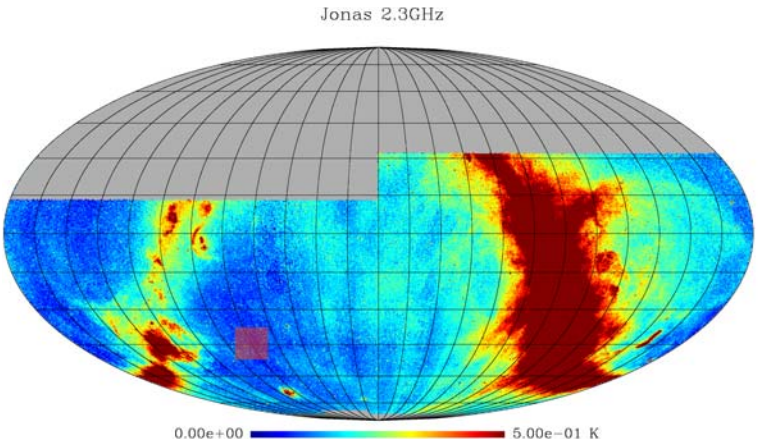

Fig. 3. Rhodes/HartRAO 2326 MHz radio continuum survey in total intensity (Jonas et al. 1999). The map is in celestial coordinates with RA=$0^{\rm h}$ in the middle. The purple square identifies the region described in this work.

synchrotron emission area of the southern sky (see Figure 3 and Carretti et al. (2002) for details about the analysis). However, no polarization observations were available for this part of the sky.

In order to fill this gap, we have observed this interesting region at 1.4 GHz (Bernardi et al. 2003) using the Australia Telescope Compact Array (Frater, Brooks & Whiteoak 1992), an east–west synthesis interferometer situated near Narrabri (NSW, Australia), operated by CSIRO–ATNF. The results and all the details of the observations are presented in Bernardi et al. (2003) and here we report the summary. The data set is arranged in a 49 pointing mosaic, which covers a $3^\circ \times 3^\circ$ region centred at the coordinate RA $= 5^{\rm h}$ and DEC $= -49^\circ$. The EW214 configuration has been used, providing sensitivity on scales ranging from $\sim 30'$ down to the angular resolution of $\sim 3\farcm4$. The system provides the four Stokes parameters I, Q, U, V. All the relevant details of the observations are listed in Table 1.

Table 1. Main characteristics of the 1.4 GHz observations

Central Frequency	1380 MHz
Effective Bandwidth	205 MHz
Array Configuration	EW214
Sensitivity Range	$3\farcm4 - 30'$
Area Position	RA $= 5^{\rm h}$, DEC $= -49^\circ$
Area Size	$3^\circ \times 3^\circ$
Observation Period	June 2002
Effective Observing Time	~ 70 h
Sensitivity per beam	0.18 mJy beam^{-1}
Sensitivity per beam	3.2 mK

The polarization maps (intensity and angles) are shown in Figure 4. The polarized emission I^p presents a patchy structure distributed over the whole field. However, a bright feature appears like a filament in the south-west corner of the area with an extension of $\sim 1^\circ$ in declination. The Stokes I image (Figure 5) does not show any particular diffuse structure at the same coordinates even though the strong point-source contamination makes the comparison difficult.

A *Faraday screen* is likely acting along the line of sight as a small-scale modulation of a relatively uniform background, transferring the power from larger to smaller scales (for a comprehensive discussion see Tucci et al. (2002), and Wieringa et al. (1993), Gaensler et al. (2001)). Our data show a uniformity scale for polarization angles of $10'$–$15'$ and we checked that this results in a power increase of Q and U on the $3'$–$30'$ scales to which the interferometer is sensitive. In the light of this the detected signal represents an upper limit of the polarized synchrotron emission in the range where the CMBP

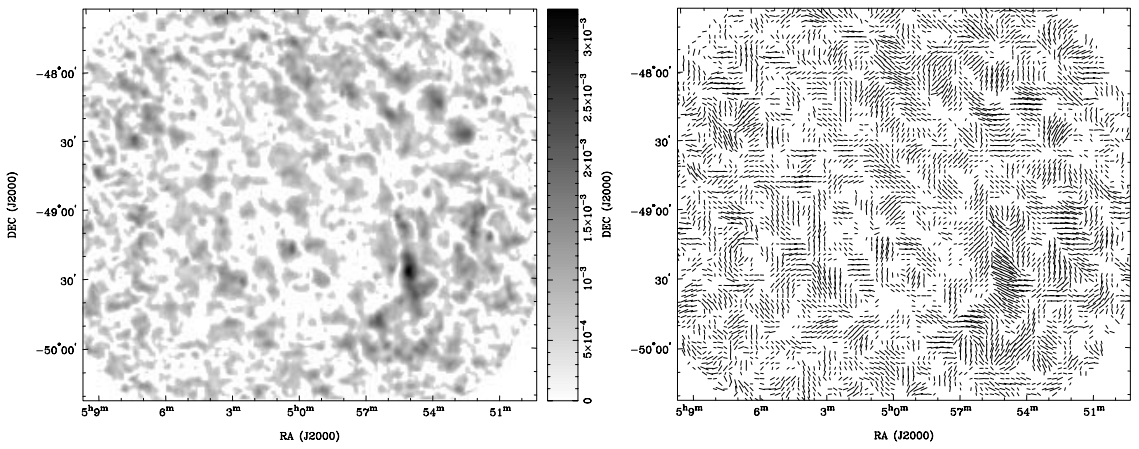

Fig. 4. Polarization maps of the observed region at 1.4 GHz: polarized total intensity I^p (left); polarization angles (right). Values are Jy beam^{-1}.

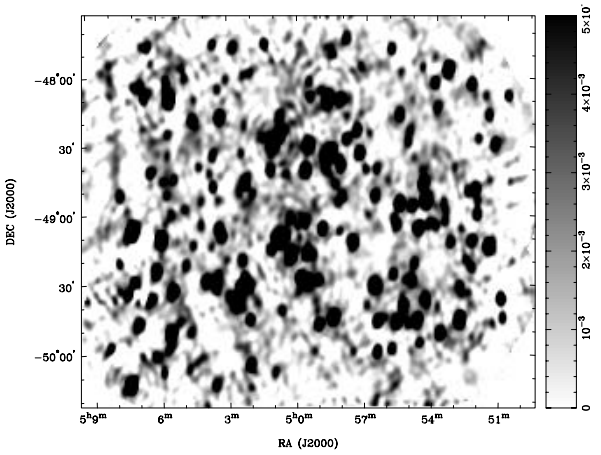

Fig. 5. Total intensity I map of the observed region at 1.4 GHz. Values are Jy beam^{-1}.

peaks ($\sim 5'$–$30'$). *Faraday screens*, therefore, do not influence the evaluation of the mean polarized emission, because they produce only a power transfer from large to small scales.

The typical Faraday rotation amount is around $|\mathrm{RM}| \sim 50$ rad/m^2, consistent with RM measurements from extragalactic radio sources (Simard–Normandin & Kronberg 1980) who find values between 30 and 60 rad/m^2 at about the same latitudes. This limits the bandwidth depolarization to $p \sim 0.92$, which is insignificantly different from 1 for our purposes of estimating the mean polarized synchrotron emission in the field.

To estimate the mean polarized synchrotron emission, we computed *rms* values of the polarized intensity I^p and of the Stokes parameters Q and U. The results, corrected for the *rms* noise contribution and restricted to the central highest sensitivity $2^\circ \times 2^\circ$ sub–field, are

$$\begin{aligned} Q_{\mathrm{rms}} &\sim 8.1 \pm 0.4 \text{ mK} \\ U_{\mathrm{rms}} &\sim 8.4 \pm 0.4 \text{ mK} \\ I^p_{\mathrm{rms}} &\sim 11.6 \pm 0.6 \text{ mK} \end{aligned} \quad (1)$$

where the error budget is dominated by the calibrator accuracy. It is worth noting that this value is nearly one order of magnitude lower than the 100–200 mK background emission found near the Galactic Plane by Uyaniker et al. (1999) at the same frequency of 1.4 GHz.

3 Effects on CMBP Measurements

We extrapolate the polarized emission found in the field to estimate the mean polarized signal at the frequencies of both BaR–SPOrt and BOOMERanG experiments by using the typical spectral index $\beta = -3.1$ found by Bernardi et al. (2004) for the synchrotron emission in the 1.4–23 GHz range. Table 2 shows the signal expectation at 32, 90 and 150 GHz as estimated after the conversion to CMB thermodynamic temperature.[1]

Table 2. Estimated synchrotron foreground noise values at frequencies of cosmological interest

ν (GHz)	Mean polarized signal (μK)
32	0.7
90	0.04
150	0.01

Since the CMBP signal is expected to be a few μK on sub–degree angular scales, both from theoretical predictions (Zaldarriaga et al. 1997) and from the recent DASI result (Kovac et al. 2002), our P_{rms} estimate suggests that in this patch the polarized synchrotron emission would not prevent the detection of the CMBP already at a frequency of 32 GHz.

The 90 GHz value is even more encouraging with the estimated synchrotron contamination two orders of magnitude lower than the predicted CMBP signal. Therefore, it is likely to measure CMBP without foreground contamination. Also, this conclusion should not be affected by the uncertainties in the synchrotron spectral index. In fact, assuming an uncertainty of ~ 0.2, we obtain a worst case foreground signal of ~ 0.08 μK, comfortably well below CMBP expectations. Considering that the new WMAP results show a steepening of ~ 0.5 in the synchrotron spectral index between K and Q bands (Bennett et al. 2003), our estimate appears to be conservative, expecially at 90 and 150 GHz.

The contamination at 150 GHz is even lower, though at this frequency the limit to the CMBP detectability is driven by the dust emission.

These results are interesting also for the B-mode. Its very low level ($I^p_{\rm rms} < 0.3$ μK for $T/S < 1$) makes the foreground contamination even more important than for the E-mode, and selected patches of the sky with low Galactic emission have to be identified to attempt the detection. Our results provide an upper limit of the Galactic synchrotron emission in the $3'$–$30'$ range and cannot be directly compared to the B-mode, which peaks on a 2° scale. However, the emission level on a certain scale is related to the APS by

$$I^p_{\rm rms} \propto \ell^2 C_\ell. \tag{2}$$

Since the Galactic synchrotron APS follows a power law $C_\ell \propto \ell^{-\alpha}$ with $\alpha < 2$ (see Figure 6), the emission we measure in the $3'$–$30'$ range represents an upper limit of the Galactic synchrotron contamination both on 2° scales and, in turn, on the B-mode.

The polarized synchrotron emission estimated at 90 GHz in this area (~ 0.04 μK) corresponds to the B–mode signal in models with $T/S \sim 0.01$, suggesting us the sensitivity for this cosmological parameter achievable in this low foreground emission area. It is worth noting that this result should be an upper limit of the contamination in this area which, therefore, appears to be a candidate for CMBP B-mode investigations.

This work is part of an activity aimed at investigating the Galactic synchrotron properties in low emission areas. Apart from a more complete analysis of this data set (e.g. APS computation), we already performed observations of the same region at 2.3 GHz. Furthermore, we have observed in June 2003 the patch target of the DASI experiment. Finally, we have successfully observed and analyzed a region in the northern sky: the northern target of BaR-SPOrt. Observations have been done with the Effelsberg telescope in collaboration with E. Fürst, P. Reich and W. Reich (MPIfR

[1] We use the conversion factor $c = \left(\frac{2\sinh\frac{x}{2}}{x}\right)^2$, where $x \equiv h\nu/kT_{cmb} \approx \nu/56.8$ GHz.

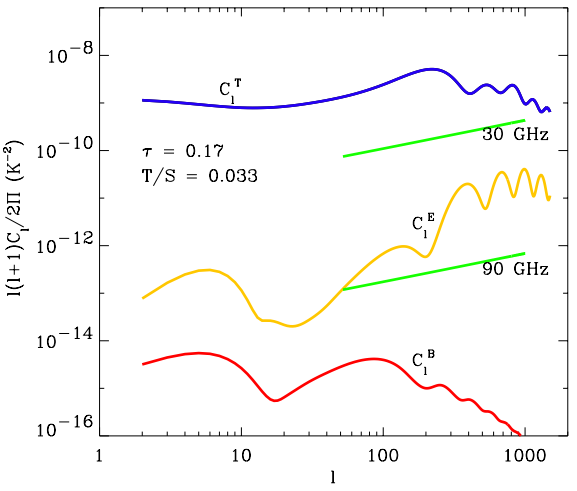

Fig. 6. Extrapolation to 30 and 90 GHz of the APS of Galactic synchrotron emission on the Galactic Plane computed by Bruscoli et al. (2002) from 2.4–2.7 GHz data (green solid line). As a reference, CMB APSs with cosmological parameters of the *Concordance Model* as from WMAP data are reported.

Bonn). Preliminary results are already available and will be subject of a forthcoming paper (Carretti et al. 2004).

Acknowledgments

This work has been carried out in the frame of BaR-SPOrt, an experiment funded by the Agenzia Spaziale Italiana (ASI). G.B. acknowledges a PhD ASI grant. We thank J.L. Jonas for providing us Rhodes/HartRAO 2326 MHz survey and acknowledge the use of the CMBFAST and HEALPix packages.

References

Bennett C.L. et al. (2003) *Astrophys. J. Suppl.* **148**, 97.
Bernardi G., Carretti E., Cortiglioni S., Sault R.J., Kesteven M.J., Poppi S. (2003) *Astrophys. J.* **594**, L5.
Bernardi G., Carretti E., Fabbri R., Sbarra C., Poppi S., Cortiglioni S., Jonas J.L. (2004) *Mon. Not. R. Astron. Soc.*, submitted.
Bruscoli M., Tucci M., Natale V., Carretti E., Fabbri R., Sbarra C., Cortiglioni S. (2002) *New Astronomy* **7**, 171.
Carretti E. et al. (2002) in *Experimental Cosmology at Millimeter Wavelengths*, Eds. M. de Petris & M. Gervasi, AIP Conf. Proc. **616**, p. 140.
Carretti E. et al. (2004) in preparation.
Cortiglioni S. et al. (2003) in *16th ESA Symposium on European Rocket and Balloon Programmes and Related Researches*, ESA Proceedings **SP-530**, p. 271.
de Bernardis P. et al. (2000) *Nature* **404**, 955.
Frater R.H., Brooks J.W., Whiteoak J.B. (1992) *Electrical Electron. Eng. Australia* **12**, 103.
Gaensler B.M., Dickey J.M., McClure–Griffiths N.M., Green A.J., Wieringa M.H., Haynes R.F. (2001) *Astrophys. J.* **549**, 959.
Jonas J.L., Baart E.E., Nicolson G.D. (1998) *Mon. Not. R. Astron. Soc.* **297**, 977.
Kamionkowski M., Kosowsky A. (1998) *Phys. Rev.* D **57**, 685.
Kogut A. et al. (2003) *Astrophys. J. Suppl.* **148**, 161.
Kovac J. et al. (2002) *Nature* **420**, 772.
Kosowsky A. (1999) *New Astron. Rev.* **43**, 157.
Simard–Normandin M., Kronberg P.P. (1980) ApJ **242**, 74.
Spergel D.N. et al. (2003) *Astrophys. J. Suppl.* **148**, 175.
Tegmark M., Eisenstein D.J., Hu W., de Oliveira-Costa A. (2000) *Astrophys. J.* **530**, 133.
Tucci M., Carretti E., Cecchini S., Nicastro L., Fabbri R., Gaensler B.M., Dickey J.M., McClure–Griffiths N.M. (2002) *Astrophys. J.* **579**, 607.
Uyaniker B., Fürst E., Reich W., Reich P., Wielebinski R. (1999) *Astron. Astrophys. Suppl.* **138**, 31.
Wieringa M.H., de Bruyn A.G., Jansens D., Brouw D.N., Katgert P. (1993) *Astron. Astrophys.* **268**, 215.
Zaldarriaga M., Spergel D.N., Seljak U. (1997) *Astrophys. J.* **488**, 1.

"The Magnetized Interstellar Medium"
8–12 September 2003, Antalya, Turkey
Eds.: B. Uyaniker, W. Reich & R. Wielebinski

A Template of Galactic Polarized Synchrotron Emission in the Frame of CMBP Experiments

G. Bernardi[1,2,3], E. Carretti[1], R. Fabbri[4], C. Sbarra[1], S. Poppi[5] and S. Cortiglioni[1]

[1]I.A.S.F./C.N.R. Bologna, Via Gobetti 101, I-40129 Bologna, Italy
[2]Dipartimento di Astronomia, Università degli Studi di Bologna, Via Ranzani 1, I-40127 Bologna, Italy
[3]ATNF/CSIRO, P.O. BOZ 76, EPPING, NSW, 1710, Australia
[4]Dipartimento di Fisica, Università di Firenze, Via Sansone 1, I-50019 Sesto Fiorentino (FI), Italy
[5]I.R.A./C.N.R. Bologna, Via Gobetti 101, I-40129 Bologna, Italy

Abstract. We present a method to model the polarized Galactic synchrotron emission in the microwave range (20–100 GHz), where this radiation is expected to play the leading role in contaminating Cosmic Microwave Background (CMB) data. Our method is based on real surveys and aims at providing the real spatial distributions of both polarized intensity and polarization angles. Its main features are the modelling of a polarization horizon to determine the polarized intensity and the use of starlight optical data to model the polarization angle pattern. Our template is virtually free of Faraday rotation effects as required at cosmological window frequencies.

1 Introduction

Recent DASI (Kovac et al. 2002) and WMAP measurements (Kogut et al. 2003) of the Cosmic Microwave Background Polarization (CMBP) highlighted the importance of studying the polarized emission of foregrounds. In fact, a sound measurement of CMBP requires good knowledge of polarized foregrounds (both Galactic and extragalactic) which are potentially more dangerous than in total intensity.

Among the polarized foreground components, the Galactic synchrotron radiation is expected to be the most relevant up to 100 GHz. In spite of its importance, synchrotron emission is scarcely surveyed: existing data mainly cover the Galactic Plane area at frequencies up to 2.7 GHz (Duncan et al. 1997; Duncan et al. 1999; Uyaniker et al. 1999; Gaensler et al. 2001; Landecker et al. 2002), far away from the 30–150 GHz frequency band which is usually considered as the cosmological window. Only the Leiden data (Brouw & Spoelstra 1976) cover high Galactic latitudes, but are limited to < 1.4 GHz and are largely undersampled.

This lack of data both in the CMB frequency range and at high Galactic latitudes can be partially recovered by building templates of the synchrotron polarized emission. Template maps would allow reliable numerical simulations to set–up and test destriping techniques as well as foreground separation methods (Revenu et al. 2000; Sbarra et al. 2003; Tegmark et al. 2000 and references therein) and could substantially help to clean CMB maps from foreground contamination (e.g. see Bennett et al. 2003).

Here we summarize the approach to model the Galactic polarized synchrotron emission in the 20–100 GHz range fully described in Bernardi et al. (2003). The method is based on real surveys and fitted to the real spatial distribution of both polarized intensity and polarization angles. Low–frequency data are used to model the polarized intensity, and optical starlight is used to model polarization angles. This allows the construction of Q and U maps covering about half of the sky with the SPOrt experiment (Cortiglioni et al. 2003) angular resolution (FWHM = 7°).

The great advantage of this approach is to produce Q and U maps free from Faraday rotation, allowing a direct extrapolation to the cosmological window.

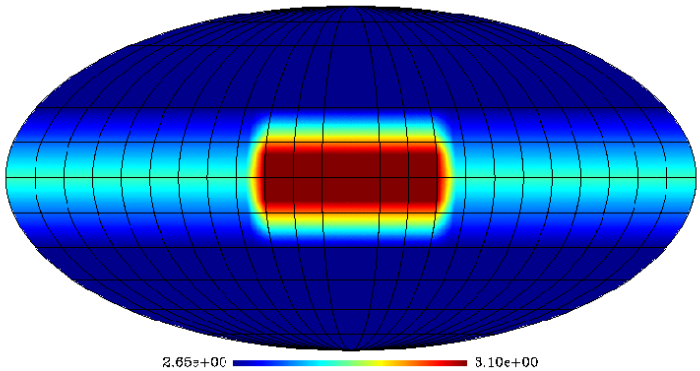

Fig. 1. Synchrotron spectral index map in the 0.408–1.4 GHz range. A steep $\beta = 3.1$ spectral index is observed towards the Galactic centre, a moderately steep spectrum ($\beta = 2.8$) relies on the Galactic Plane and a flatter one ($\beta = 2.65$) at high Galactic latitude.

2 The Model

To generate Q and U template maps of the Galactic synchrotron polarized radiation in the 20–100 GHz range, we need two ingredients:

1. a polarized intensity (I_p) map which can be obtained from existing total intensity (I) sky surveys assuming a model to link the polarized to the total intensity synchrotron emission after cleaning the free–free component;

2. a polarization angle map not affected by Faraday rotation.

The first requirement can be fulfilled by using the 0.408 GHz Haslam et al. map (Haslam et al. 1982) and the 1.4 GHz Reich map (Reich 1982; Reich & Reich 1986) to provide a pure total–intensity synchrotron map clean from free–free emission. Such emission is not negligible in low–frequency data, in particular in the Galactic Plane (see also Reich & Reich 1998) and must be subtracted off.

The second requirement can be fulfilled by using the Heiles starlight polarization catalogue (Heiles 2000), starlight data being virtually free of Faraday rotation. A complete polarization angle map can be obtained interpolating the sparse starlight data.

2.1 The Polarized Intensity Map

Free–free subtraction from the low–frequency radio surveys is performed by applying a modified Dodelson (1997) technique which takes into account the different spectral behaviours of synchrotron and free–free radiations.

In the Dodelson formalism a scalar product is defined for vectors, whose normalization is based on the CMB shape (see Dodelson (1997) for details). We modify it by using the free–free shape.

The subtraction procedure requires the knowledge of the synchrotron and free–free spectral indices. For the latter we adopt $\beta = 2.1$ (Reich & Reich 1988), whereas for the synchrotron radiation we derive a simple model for its spatial variation based on the Reich & Reich (1988) analysis (Figure 1).

The separation procedure results in a pure total intensity synchrotron map which can be converted into a polarized intensity map providing a relation between total and polarized intensities.

We assume the existence of a *polarization horizon* (Duncan et al. 1997; Duncan et al. 1999; Landecker et al. 2002; Gaensler et al. 2001), that is a sort of bubble centred in the observer position: the observed polarized signal comes from integration along the line of sight out to the horizon, whereas the signal beyond it is depolarized by variations of polarization angles (changes in the Galactic magnetic field). The size of the horizon is not yet known: it depends on several effects along the line of sight, like Galactic magnetic field turbulence and electron density variations. However, it has been suggested

that it may range from 2 kpc (Gaensler et al. 2001) up to 7 kpc (Duncan et al. 1997; Landecker et al. 2002), so that a few kpc appear to be an acceptable estimate.

This polarization horizon allows us to model the relation between polarized and total intensity synchrotron emission. Given the mean total synchrotron emissivity $J^s(\nu, l, b)$ at Galactic coordinates (l, b) as well as the thickness $L(l, b)$ of the synchrotron emitting region in the same direction, the brightness temperature $T^s(\nu, l, b)$ at frequency ν is:

$$T^s(\nu, l, b) = \frac{c^2}{2K\nu^2} J^s(\nu, l, b)\, L(l, b)\ , \tag{1}$$

where K is the Boltzmann constant. The thickness $L(l, b)$ depends on the geometrical model describing the space distribution of the relativistic–electron gas responsible for synchrotron emission. We consider the simplest case where the gas is uniformly distributed in the Galactic halo represented by a sphere of radius $R = 15$ kpc centred into the Galactic Centre (GC). Thus the thickness $L(l, b)$ is the distance between the Sun and the edge of this sphere:

$$L(l, b) = d\, \cos(b)\, \cos(l) \left[1 + \sqrt{1 + \frac{(R^2/d^2 - 1)}{\cos^2(b)\, \cos^2(l)}}\right]\ , \tag{2}$$

where $d = 9$ kpc is the Sun's distance from the GC (see Bernardi et al. (2003) for details).

Similarly, the polarized brightness temperature T_p^s can be defined provided the emission is integrated out to the polarization horizon R_{ph} and a polarization degree p is introduced:

$$T_p^s(\nu, l, b) = \frac{c^2}{2K\nu^2}\, p\, J^s(\nu, l, b)\, R_{ph}\ . \tag{3}$$

Finally, equations (1) and (3) provide the relation between polarized and total intesity emissions:

$$T_p^s(\nu, l, b) = p \frac{R_{ph}}{L(l, b)} T^s(\nu, l, b)\ . \tag{4}$$

The quantity $p\, R_{ph}$ is unknown and represents a free parameter to be calibrated with real data.

2.2 Polarization Angle Map

Since at microwave frequencies Faraday rotation effects become negligible (Bernardi et al. 2003), the distribution of polarization angles cannot be derived directly from existing low–frequency radio surveys due to the presence of a relevant amount of Faraday rotation.

Brown & Taylor (2001) estimate a typical Rotation Measure (RM) of the Galactic Plane as RM $= -183 \pm 14\ \cos(l - 84^\circ \pm 4^\circ)$ rad m^{-2}, which means that the polarization angle can be rotated up to $|160^\circ|$ at 2.7 GHz, which is the survey with the highest frequency available (Duncan et al. 1999).

To overcome this problem we use the Heiles catalogue of starlight polarization, the optical frequencies being unaffected by Faraday rotation. The polarization vector of starlight is parallel to the Galactic magnetic field **B** because of selective absorption by interstellar dust grains, whose minor axis is aligned with **B** (Fosalba et al. 2001). Since the synchrotron polarization vector is perpendicular to **B**, starlight polarization angles can be used as a template for polarization angles provided a 90° rotation is performed. Also, starlight polarization has the great advantage of sampling the high Galactic latitude regions not present in low–frequency polarization surveys.

Most of the Heiles catalogue stars ($\simeq 87\%$) are within 2 kpc, tracking the local magnetic field. Their distance is of the order of the polarization horizon size, confirming that the Heiles catalogue can be safely used as a template for the polarization angles of synchrotron emission.

Since starlight polarization angles are irregularly distributed (Figure 2), we fill data holes by linear interpolation. We perform the interpolation by generating Q, U pairs corresponding to the Heiles polarization angles θ:

$$Q_\theta = \cos(2\theta) \qquad U_\theta = \sin(2\theta). \tag{5}$$

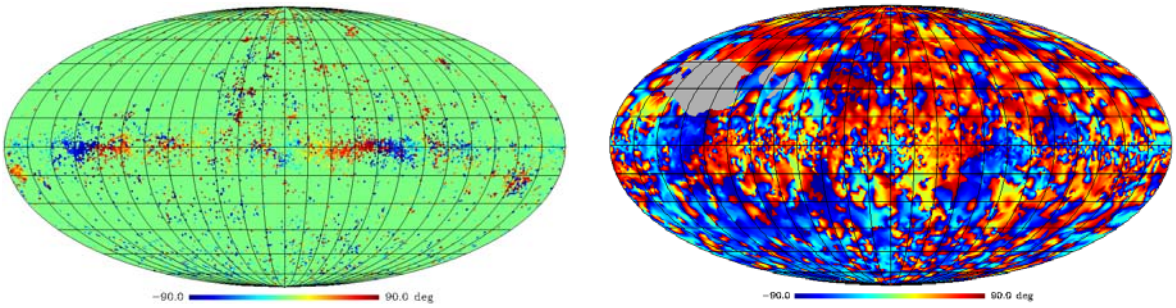

Fig. 2. Left: Map of starlight polarization angles. Right: Interpolated map of starlight polarization angles.

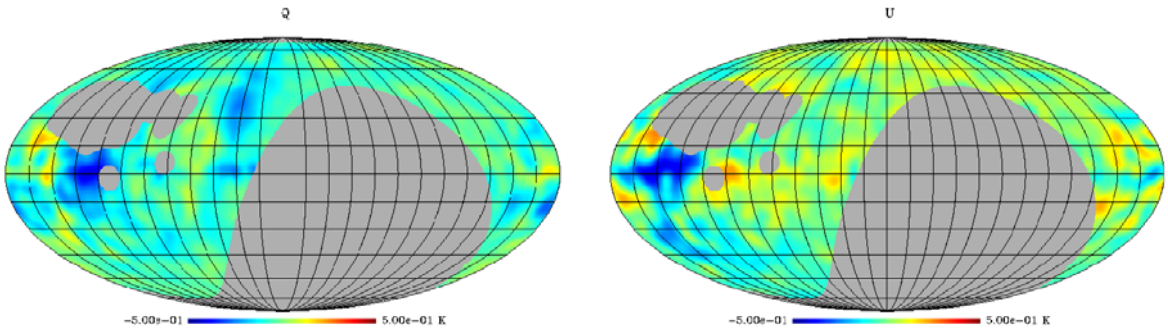

Fig. 3. Left: Template map of the Stokes parameter Q at 1.4 GHz with a 7° resolution. Right: The same but for the Stokes parameter U.

Then, for each pixel of the template map to be built we linearly interpolate the Q_θ and U_θ values of the three closest stars and compute the corresponding polarization angle; the interpolated map is shown in Figure 2. The interpolation method uses parallel transport as described in Bruscoli et al. (2002).

3 Results

Our results are shown in Figure 3, where the Q and U templates at 1.4 GHz are presented. Figure 4 shows a comparison between the polarized intensity I_p of our model and the I_p map obtained from the Brouw & Spoelstra (1976) data. The comparison is done only for I_p because polarization angles are strongly affected by Faraday rotation at 1.4 GHz. Our template is able to reproduce the basic and brightest structures in the Brouw & Spoelstra (1976) data like the *Fan region* and the North Galactic Spur, though the latter is fainter than in real data.

The good agreement between the map obtained from the Brouw & Spoelstra (1976) data and our model allows us to calibrate the parameter $p\,R_{ph}$ by matching the I_p emission of the two maps in a well defined area. We use the Fan region, the most defined and morphologically similar area in both maps. The calibration uses the 820 MHz Brouw & Spoelstra (1976) data (see Figure 2 in Bruscoli et al. 2002) rather than those at 1.4 GHz, because of their better sampling, providing

$$p\,R_{ph} = 0.9 \pm 0.09 \text{ kpc} \ . \tag{6}$$

Assuming the polarization degree p on 7° scales is in the range ~ 0.15–0.3 (Tegmark et al. 2000) we obtain for the polarization horizon $3\,\text{kpc} < R_{ph} < 6\,\text{kpc}$, in good agreement with present estimates (Duncan et al. 1997; Gaensler et al. 2001; Landecker et al. 2002).

We extrapolate the Q and U templates at 1.4 GHz to the cosmological window, and in particular to the frequencies of 22, 32, 60 and 90 GHz which are of interest for the SPOrt experiment. We use a power law with the mean synchrotron spectral index $\beta = 3.0$ found by Platania et al. (1997) in the

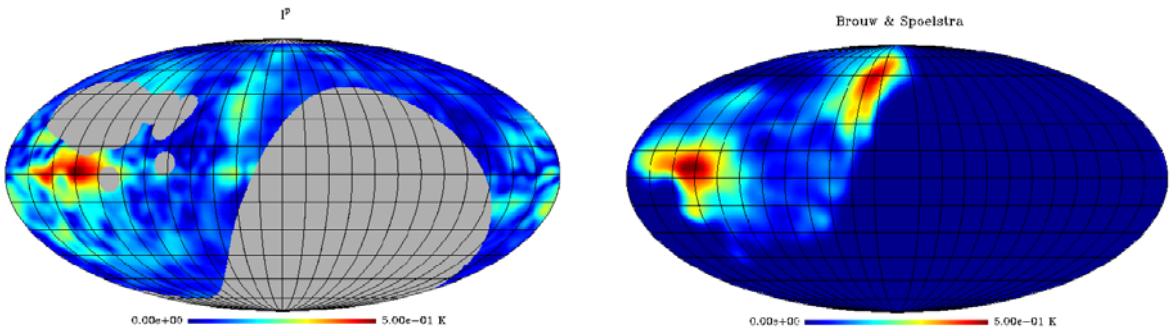

Fig. 4. Left: Template map of the polarized intensity I_p at 1.4 GHz with 7° resolution. Right: Map of the polarized intensity I_p at 1.4 GHz obtained from the Brouw & Spoelstra data and convolved with a FWHM = 7° Gaussian beam.

Table 1. Peak emission (*Fan region*) and $P_{\rm rms}$ of our template at the four SPOrt frequencies. The $P_{\rm rms}$ is computed on the low emission areas (the faintest 50% pixels).

ν (GHz)	$I_{p,\rm max}$ (μK)	$P_{\rm rms}$(μK)
1.4	5×10^5	6.6×10^4
22	130	17
32	43	5.6
60	6.5	0.84
90	1.9	0.25

1–19 GHz range. In Table 1 we report the emission of the most important structure (the Fan region) and the mean polarization level $P_{\rm rms} = \sqrt{\langle Q^2 \rangle + \langle U^2 \rangle}$ of the low–emission areas (the faintest 50% pixels) for all the SPOrt frequencies.

4 Conclusions

We have presented a method to build template maps of the polarized Galactic synchrotron emission free from Faraday rotation effects, which can be safely extrapolated to the cosmological–window frequency range. Differing from previous spatial models (Giardino et al. 2002; Kogut & Hinshaw 2000), our template is intended to provide the real spatial distribution of both polarized intensity and polarization angles. Most previous work adopted a complementary approach based on angular frequency rather than real space (Tucci et al. 2000, 2002; Baccigalupi et al. 2001; Giardino et al. 2002; Bruscoli et al. 2002) where the angular power spectra of the polarized synchrotron foreground were computed for low–frequency data and then extrapolated to high frequency. Such extrapolation is not trivial due to Faraday rotation, affecting low–frequency data and being negligible in the cosmological window.

The template developed here is intended to overcome such a problem: polarization angular spectra in the cosmological window should be computed on the spatial template rather than simply extrapolated from the direct analysis of low–frequency maps.

Template maps obtained with the present method still suffer from the uncertainties in the extrapolation due to our ignorance of the synchrotron spectrum. In order to minimize such uncertainties, template maps of the synchrotron polarized emission should be directly at microwave frequencies, as is now possible thanks to WMAP latest total intensity maps (Bennett et al. 2003). Such a work is the subject of a forthcoming paper (Bernardi et al. 2004).

Acknowledgments

This work has been carried out in the frame of the SPOrt experiment, a programme funded by ASI. G.B. acknowledges a Ph.D. ASI grant. We ackonwledge the use of the HEALPix package.

References

Baccigalupi C., Burigana C., Perrotta F., De Zotti G., La Porta L., Maino D., Maris M., Paladini R. (2001) *Astron. Astrophys.* **372**, 8.
Bennett C.L. et al. (2003) *Astrophys. J. Suppl.* **148**, 97.
Bernardi G., Carretti E., Fabbri R., Sbarra C., Poppi S., Cortiglioni S. (2003) *Mon. Not. R. Astron. Soc.* **344**, 347.
Bernardi G., Carretti E., Fabbri R., Sbarra C., Poppi S., Cortiglioni S. (2004) *Mon. Not. R. Astron. Soc.*, submitted.
Brouw W.N., Spoelstra T.A.T. (1976) *Astron. Astrophys. Suppl.* **26**, 129.
Brown J.C., Taylor A.R. (2001) *Astron. J.* **563**, L31.
Bruscoli M., Tucci M., Natale V., Carretti E., Fabbri R., Sarra C., Cortiglioni S. (2002) *New Astron.* **7**, 171.
Cortiglioni et al. (2003) *New Astron.*, in press.
Dodelson S. (1997) *Astrophys. J.* **482**, 577.
Duncan A.R., Haynes R.F., Jones K.L., Stewart R.T. (1997) *Mon. Not. R. Astron. Soc.* **291**, 279.
Duncan A.R., Reich P., Reich W., Fürst E. (1999) *Astron. Astrophys.* **350**, 447.
Fosalba P., Lazarian A., Prunet S., Tauber J.A. (2002) *Astrophys. J.* **564**, 762.
Gaensler B.M., Dickey J.M., McClure-Griffiths N.M., Green A.J., Wieringa M.H., Haynes R.F. (2001) *Astrophys. J.* **549**, 959.
Giardino G., Banday A.J., Gorsky K.M., Bennet K., Jonas J.L., Tauber J.A. (2002) *Astron. Astrophys.* **387**, 82.
Haslam C.G.T., Stoffel H., Salter C.J., Wilson W.E. (1982) *Astron. Astrophys. Suppl.* **47**, 1.
Heiles C. (2000) *Astron. J.* **119**, 923.
Kogut A., Hinshaw G. (2000) *Astrophys. J.* **543**, 530.
Kogut A. et al. (2003) *Astrophys. J. Suppl.* **148**, 161.
Kovac J., Leitch E.M., Pryke C., Carlstrom J.E., Halverson N.W., Holzapfel W.L. (2002) *Nature* **420**, 772.
Landecker T.L., Uyanıker B., Kothes R. (2002) in *Astrophysical Polarized Backgrounds*, eds. S. Cecchini, S. Cortiglioni, R. Sault, C. Sbarra, AIP Conf. Proc. **609**, p. 9.
Reich P., Reich W. (1986) *Astron. Astrophys. Suppl.* **63**, 205.
Reich P., Reich W. (1988) *Astron. Astrophys. Suppl.* **74**, 7.
Reich W. (1982) *Astron. Astrophys. Suppl.* **48**, 219.
Revenu B., Kim A., Ansari R., Couchot F., Delabrouille J., Kaplan J. (1982) *Astron. Astrophys. Suppl.* **142**, 499.
Sbarra C., Carretti E., Cortiglioni S., Zannoni M., Fabbri R., Macculi C., Tucci M. (2003) *Astron. Astrophys.* **401**, 1215.
Tegmark M., Eisenstein D.J., Hu W., de Oliveira-Costa A. (2000) *Astrophys. J.* **530**, 133.
Tucci M., Carretti E., Cecchini S., Fabbri R., Orsini M., Pierpaoli E. (2000) *New Astron.* **5**, 181.
Tucci M., Carretti E., Cecchini S., Nicastro L., Fabbri R., Gaensler B.M., Dickey J.M., McClure-Griffiths N.M. (2002) *Astrophys. J.* **579**, 607.
Uyanıker B., Fürst E., Reich W., Reich P., Wielebinski R. (1999) *Astron. Astrophys. Suppl.* **138**, 31.